Mechanics and dynamics of biopolymer networks

Broedersz, C.P.

2011

document version
Publisher's PDF, also known as Version of record

3

Elasticity of semiflexible polymer networks with flexible cross-links

- C. P. Broedersz, C. Storm and F. C. MacKintosh
  Nonlinear elasticity of composite networks of stiff biopolymers with flexible linkers,
  Physical Review Letters, **101**: 118103 (2008)

- C. P. Broedersz, C. Storm and F. C. MacKintosh
  Effective medium approach for stiff polymer networks with flexible cross-links,
  Phys. Rev. E **79**, 061914 (2009)

Abstract

Recent experiments have demonstrated that the nonlinear elasticity of *in vitro* networks of the biopolymer actin is dramatically altered in the presence of a flexible cross-linker such as the cytoskeletal protein filamin. The basic principles governing the mechanical properties of such networks, however, remain poorly understood. Here we describe an effective medium theory of flexibly cross-linked stiff polymer networks. The network is modeled as a collection of randomly oriented rods connected by flexible cross-links to an elastic continuum. This effective medium is treated in a linear elastic limit as well as in a more general framework, in which the medium self-consistently represents the nonlinear network behavior. This model predicts that the nonlinear elastic response sets in at strains proportional to cross-linker length and inversely proportional to filament length. Furthermore, we find that the differential modulus scales linearly with the stress in the stiffening regime. These results are in excellent agreement with bulk rheology data.

3.1 Introduction

The mechanical response and locomotion of living cells is mainly controlled by the cellular cytoskeleton. The cytoskeleton is a highly composite network of various stiff biopolymers, along with various binding proteins for force generation, cross-linking and polymer growth regulation. Understanding the basic physics that governs the mechanical properties of a composite biopolymer network represents an important biophysical challenge that will help elucidate the mechanics of a living cell. In addition to their importance for cell mechanics, cytoskeletal networks have also demonstrated novel rheological properties, especially in numerous *in vitro* studies [1–10]. However, there have been few theoretical or experimental studies that address the composite nature of the cytoskeleton [11–16]. Recent experiments on F-actin networks with the highly compliant cross-linker filamin, in particular, have demonstrated several striking features: These networks can have a linear modulus as low as 1 Pa, which is significantly lower than for actin gels with incompliant cross-links, and yet they can withstand stresses of 100 Pa or more and can stiffen dramatically by up to a factor of 1000 under applied shear [10, 11]. Both the linear and nonlinear elastic properties of actin-filamin gels appear to be dramatically affected by the flexible nature of the cross-links, resulting in novel behavior as compared to actin-networks with incom-

pliant cross-links, and to synthetic polymer gels. This suggests new network design principles that may be extended to novel synthetic materials with engineered cross-links [12]. However, the basic physics of networks with flexible cross-links remain unclear.

In this chapter we provide a detailed description of an effective medium approach to describe the nonlinear elastic properties of composite networks consisting of stiff filaments linked by highly flexible cross-links [15]. A schematic image of the network we aim to model is shown in Fig. 3.1. The network is composed of randomly oriented filaments/rods of length L, which are linked together by highly flexible cross-linkers. The cross-links consist of two binding domains interconnected by a thermally fluctuating flexible polymer chain of length ℓ_0. The compliance of such a cross-linker is entropic in nature. Adopting the WLC model, we can fully characterize the cross-linkers with a contour length ℓ_0 and a persistence length ℓ_p [17, 18]. The WLC force-extension curve becomes highly nonlinear when the cross-linker reaches its full extension, as shown in Fig. 3.2 c). Indeed, atomic force microscope (AFM) measurements show that an actin cross-linker such as filamin exhibits strain stiffening and can be accurately described as a wormlike chain (WLC) [24, 25]. At large mechanical loads, however, the experimental force-extension curve deviates significantly from WLC behavior. The polymer chain in cross-linkers such as filamin consists of repeated folded protein domains, which unfold reversibly at sufficiently large mechanical loads. The experiments by Furuike et al. [25] show that after an initial stiffening regime at a force-threshold of ≈ 100 pN, one of the protein domains unfolds. The accompanied increase in contour length results in a strong decrease in the cross-linkers stiffness. This softening is immediately followed by WLC stiffening as the thermal undulations of the lengthened cross-linker are stretched out. This leads to an elastic response that alternates between entropic stiffening and softening caused by domain unfolding, resulting in a sawtooth force-extension curve.

It has been suggested that the unfolding behavior of filamin plays an important role in the mechanical properties of networks with such cross-linkers [11, 13, 25]. Simulations of stiff polymer networks, assuming a sawtooth force-extension curve for the unfoldable cross-links, reveal that such networks exhibit a fragile state in which a significant fraction of cross-linkers is at the threshold of domain unfolding [13]. This results in strain softening of the network under shear, inconsistent with the pronounced stiffening response observed experimentally in actin-filamin gels [10, 11]. We estimate, however, that under typical *in vitro* experimental conditions, domain unfolding in the cross-links is highly unlikely. For domain unfolding to occur with multiple filamin crosslinks experiencing forces of order 100 pN, the resulting tension in the actin filaments is likely to exceed rupture forces of order 300 pN of F-actin [26]. Also, a simple estimate of the macroscopic stress corresponding to even a small fraction of filamins under 100 pN tensions is larger than the typical limit of shear stress

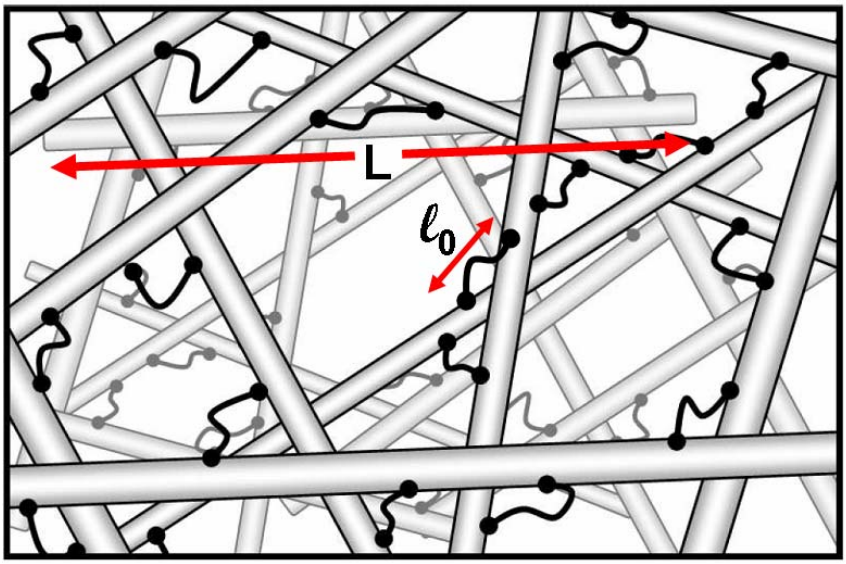

Figure 3.1 – (Color online) Schematic figure of an isotropic stiff polymer network with highly compliant cross-linkers.

before network failure is observed. Therefore, we do not expect domain unfolding to occur. Rather, it seems likely that cross-link unbinding occurs before sufficiently large sufficiently large forces are reached for domain unfolding. Detailed estimates based on experiments suggest filamin tensions only of order 1-5 pN at network failure [16]. It has also been shown in single molecule experiments [27] that filamin unbinds from F-actin at forces well below the forces required for unfolding, which indicates that cross-linker unfolding is unlikely to occur in typical network conditions. Therefore, we consider only the initial stiffening of the cross-links, which we show can account well for the observed nonlinear elasticity of actin-filamin gels.

Our model consists of a network of stiff filaments connected by flexible cross-linkers. The compliance of such a network is expected to be governed by the cross-linkers. The stiff filaments provide connectivity to the network and constrain the deformation of the cross-linkers, thereby setting the length scale of the effective unit cell of the network. Thus, we expect that the elasticity of the network will be controlled by the filament length L and network connectivity, which is expressed in terms of the number of cross-link per filament n. Therefore, we describe the network with a model in which the basic elastic element consists of a single stiff rod and many compliant cross-linkers that connect the rod to a surrounding linear elastic medium.

3.2 Effective Medium Approach

Networks of semiflexible polymers with point-like incompliant cross-links have been studied extensively [4, 5, 28–31]. These systems exhibit two distinct elastic regimes: one in which the deformation of the network is affine and a regime that is characterized by highly non-affine deformations. The network is said to deform affinely if the strain field is uniform down to the smallest length scale of the network. Simulations have shown that the deformation of these networks becomes more affine with increasing cross-link concentration and polymer length [32, 33], which has been borne out by experiments [4, 34]. The elastic response of the network can fully be accounted for by the stretching modes of the polymers in the affine regime. In addition to stretching modes, stiff polymers can also store energy in a non-affine bending mode. Indeed, it has been shown that in sparser networks, in which there are fewer constraints on the constituting polymers, non-affine bending modes dominate the elastic response [29, 32, 33]. We will, however, not consider this sparse network limit here.

In a dense network of stiff polymers with highly flexible cross-links, we expect the soft stretching modes of the linkers to govern the network elasticity. However, the large separation in size and stiffness between cross-links and filaments does imply a non-uniform deformation field for the cross-links at the sub-filament level. On a coarse-grained level the network deforms affinely and stretches the cross-links as depicted in Fig. 3.2 b. The network surrounding this particular rod is shown here as a grey background. The deformation of the cross-links increases linearly from 0 in the center towards a maximum value at the boundaries of the rod. At small strains the cross-links are very soft and follow the deformation of the stiffer surrounding medium. However, at a strain $\gamma_c \sim \ell_0/L$ the outer-most cross-links reach their full extension and, consequently, stiffen dramatically. This suggest the existence of a characteristic strain γ_c, for the onset of the nonlinear response of the network.

The macroscopic elasticity of the network results from the tensions in all the constituting filaments. The tension in a particular filament can be determined by summing up the forces exerted by the cross-links on one side of the midpoint of the filament. We will employ an effective medium approach to calculate these forces as a function of filament orientation and the macroscopic strain. Thus, we model the network surrounding one particular rod, as an affinely or uniformly deforming continuum, which effectively represents the elasticity of the network, as depicted in Fig. 3.2 a and b. We then proceed by considering contributions from rods over all orientations to calculate the macroscopic response of the network.

The remainder of this chapter is organized as follows. First we discuss a model in which the effective medium is treated as a linear elastic continuum. In this model we describe the cross-links both as linear springs with finite extension and as WLC cross-links. We analyze our model in both a fully 3D network, as well as a simplified 1D

representation, which already captures the essential physics of the nonlinear behavior. At large strains, when many of the cross-linkers are extended well into their nonlinear regime, it is no longer realistic to model the surrounding network as a linear medium. Therefore, we extend our linear medium model in a self-consistent manner, replacing the embedding medium by a nonlinear effective medium whose elastic properties are determined by those of the constituent rods and linkers. This self-consistent model can quantitatively account for the nonlinear response found in prior experiments on actin filamin networks [11, 16]. Finally, we can compute the tension profiles along the filaments and we demonstrate how to use these to express the macroscopic stress in terms of the maximum force experienced by a single cross-link, which may set the failure stress of the network.

3.3 The Linear medium model

We first develop a one dimensional representation of our model, which will be used in section 3.5 to construct a more realistic three dimensional model. Also we will restrict the treatment here to a linear description of the effective medium, a constraint that is lifted in section 3.4.

Consider a rigid rod of length L connected by n flexible cross-links to an elastic medium. We shall refer to this configuration—consisting of a rod decorated by flexible linkers—as the basic elastic unit (BEU). The medium is stretched by an externally imposed extensional strain ϵ parallel to the orientation of the rod. Throughout this chapter we denote a 1D extensional strain with ϵ and a 3D shear strain with γ. The presence of the BEU in the medium reduces the deformation of the medium at a position x in the rest frame of the rod by an amount $u_{EM}(x,\epsilon) = \epsilon x - u_{cl}(x,\epsilon)$, where $u_{cl}(x,\epsilon)$ is the extension of a cross-linker at a distance x from the center of the rod. The magnitude of $u_{cl}(x,\epsilon)$ and $u_{EM}(x,\epsilon)$ are set by requiring force balance between the cross-links and the medium.

$$f_{cl}(u_{cl}(x,\epsilon)) = K_{EM} u_{EM}(x,\epsilon), \tag{3.1}$$

where $f_{cl}(u)$ is the force-extension curve of a single cross-linker and where K_{EM} is the elastic constant of the medium. The tension τ_0 in the center of the rod is found by summing up the forces exerted by the stretched cross-links on one side of the midpoint of the rod. Assuming a high, uniform line density n/L of cross-links along the rod, we can write the sum as an integral

$$\tau_0(\epsilon) = \frac{n}{L} \int_0^{L/2} dx' \, f_{cl}\big(u_{cl}(x',\epsilon)\big). \tag{3.2}$$

where $u_{cl}(x',\epsilon)$ is obtained by solving Eqn. (3.1). The full tension profile $\tau(\epsilon, x)$ is

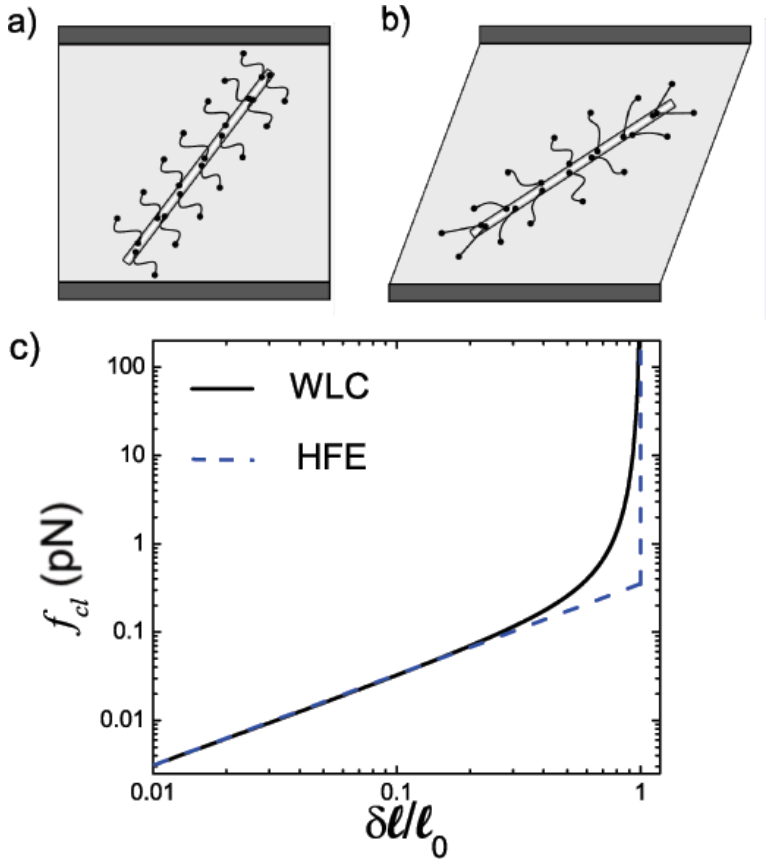

Figure 3.2 – (Color online) a) a single filament connected by n flexible cross-links to the surrounding network, which we model as an effective elastic continuum (shown here as a grey background) and b) illustrates the proposed nonuniform deformation of the cross-linkers on a single filament in a sheared background medium. c) Force-extension curve of a Hookean Finite Extendable (HFE) cross-linker (dashed blue curve) and of a WLC cross-linker (solid black curve).

found by replacing the lower limit of the integration by x

$$\tau(\epsilon, x) = \frac{n}{L} \int_x^{L/2} dx' f_{cl}\big(u_{cl}(x', \epsilon)\big) \tag{3.3}$$

3.3.1 Hookean Finite Extendable cross-linkers

We can solve Eqns. (3.1) and (3.2) to compute the midpoint tension in a rod for a specific force-extension curve for the cross-links. In the absence of unfolding or unbinding, we can describe the force-extension behavior of a flexible cross-linker such as filamin with the WLC model, as depicted with the black solid line in Fig. 3.2 c). It is instructive to simplify the WLC force-extension curve by assuming a Hookean response with a spring constant k_{cl} up to an extension ℓ_0, which is the molecular weight of the cross-linker. The spring constant $k_{cl} = \frac{2}{3}\frac{k_B T}{\ell_p \ell_0}$ is found from the WLC model for small extensions in the limit $\ell_p \ll \ell_0$ [18], where $k_B T$ is the thermal energy. Beyond an extension ℓ_0, the cross-linker becomes infinitely stiff. The force-extension curve of these Hookean Finite Extendable (HFE) cross-links is shown as a blue dashed curve in Fig. 3.2 c). The finite extensibility of the cross-links implies a critical strain $\epsilon_c = \frac{\ell_0}{L/2}$ at which the cross-linkers at the boundaries of the rod reach full extension. Since the linkers are placed in series with the medium the elastic constants add; thus, for strains $\epsilon \leq \epsilon_c$

$$\tau_0(\epsilon) = \frac{n}{L} \int_0^{L/2} dx' \, \frac{k_{cl} K_{EM}}{k_{cl} + K_{EM}} \epsilon x'. \tag{3.4}$$

Thus, the midpoint tension depends linearly on strain for $\epsilon \leq \epsilon_c$. For larger strains, the expression for the midpoint tension in the rod in Eq. (3.2) reads

$$\begin{aligned} \tau_0(\epsilon) &= \frac{n}{L} \int_0^{\ell_0/\epsilon} dx' \, \frac{k_{cl} K_{EM}}{k_{cl} + K_{EM}} \epsilon x' \\ &+ \frac{n}{L} \int_{\ell_0/\epsilon}^{\frac{L}{2}} dx' \left[\frac{k_{cl} K_{EM}}{k_{cl} + K_{EM}} \ell_0 + K_{EM}(\epsilon x' - \ell_0) \right]. \end{aligned} \tag{3.5}$$

The expression has separated into two integrals, representing a sum over the cross-links with an extension $< \ell_0$ and a sum over the cross-links that have already reached full extension. We also note that beyond ϵ_c, the midpoint tension depends nonlinearly on strain. Using Eq. (3.5) we compute the 1D modulus $G_{1D} = \tau_0/\epsilon$, as shown in Fig. 3.3. Below the critical strain, the response is dominated by the linear elasticity of the cross-links $G_{1D} \approx \frac{1}{8} n k_{cl} L$. The cross-links at the edge of the rod become rigid at a strain threshold $\epsilon_c = 2\ell_0/L$. As the strain is further increased, the cross-links stiffen consecutively (inwards from the edge of the rod), resulting in a sharp increase of G_{1D}. At large strains, G_{1D} asymptotically approaches a second linear regime $\sim \frac{1}{8} n K_{EM} L$.

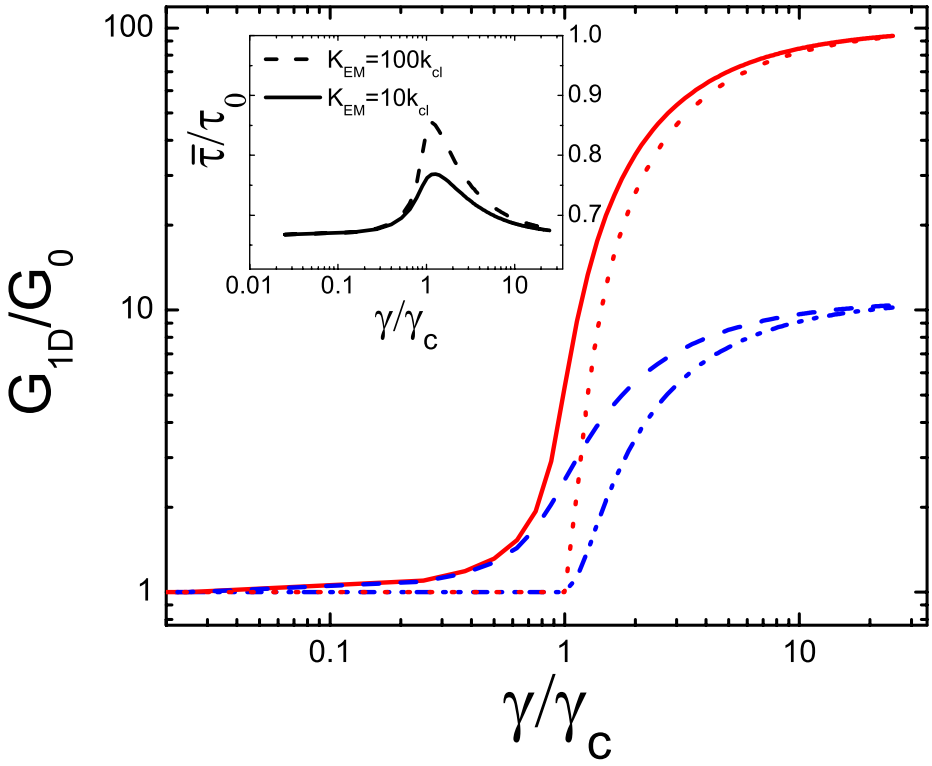

Figure 3.3 – (Color online) a) The modulus $G_{1D} = \tau_0/\epsilon$ for the 1D representation of the linear medium model with HFE cross-links with $K_{EM} = 10k_{cl}$ (blue dash dotted curve) and $K_{EM} = 100k_{cl}$ (red dotted curve). We also show G_{1D} for the model with WLC cross-links with $K_{EM} = 10k_{cl}$ (blue dashed curve) and $K_{EM} = 100k_{cl}$ (red solid curve). The inset shows the ratio of the average tension $\bar{\tau}$ and the midpoint tension τ_0.

3.3.2 Worm Like Chain cross-Linkers

We now consider flexible cross-linkers described by the more realistic WLC force-extension curve, as depicted by the solid line in Fig. 3.2 c. The force-extension relation is well described by the interpolation formula [18]

$$f_{cl}(u) = \frac{k_B T}{\ell_p}\left(\frac{1}{4\left(1-\frac{u}{\ell_0}\right)^2} - \frac{1}{4} + \frac{u}{\ell_0}\right), \tag{3.6}$$

where k_B is Boltzmann's constant and T is the temperature. This interpolation formula captures the linear and asymptotic stiffening regimes. More detailed theoretical work on WLC polymers in this limit can be found in [19–23]. Using Eqs. (3.1) and (3.2), the 1D modulus G_{1D} is calculated for cross-linkers with this force-extension curve, as shown in Fig. 3.4. The force-extension curve of the WLC cross-linker is linear up to extensions very close to ℓ_0, upon which a pronounced stiffening occurs, as shown in Fig. 3.2 c). We can use these features, together with the property that for a dense network the medium is much stiffer than the flexible cross-linkers $K_{EM} \gg k_{cl}$, to write an approximate expression for the tension in a rod in a closed form analogous to Eq. (3.5).

$$\begin{aligned}\tau_0(\epsilon) \quad &\approx \frac{n}{L}\int_0^{\ell_0/\epsilon} dx' \int_0^{\epsilon x'} du \frac{k_{cl}(u)K_{EM}}{k_{cl}(u)+K_{EM}} \\ + \quad &\frac{n}{L}\int_{\ell_0/\epsilon}^{\frac{L}{2}} dx' \left[\int_0^{\ell_0} du \frac{k_{cl}(u)K_{EM}}{k_{cl}(u)+K_{EM}} + K_{EM}(\epsilon x' - \ell_0)\right],\end{aligned} \tag{3.7}$$

where $k_{cl}(u)$ is the differential stiffness df_{cl}/du of the WLC cross-linker. This equation states that the BEU deforms essentially affine up to the critical strain. Beyond ϵ_c, those cross-links that have reached full extension are no longer compliant and start to pull back on the surrounding medium. The approximate calculation of $d\tau_0/d\epsilon$ using Eq. (3.7) is shown together with the exact calculation performed with Eq. (3.2) in Fig. 3.4. This graph demonstrates that the approximation captures the essential behavior of the exact curve, and results only in a minor quantitative difference in the cross-over regime. Therefore, we will continue constructing our model using this more convenient approximate form.

The 1D modulus calculated with Eq. (3.7) is shown for the WLC cross-links together with the results of the HFE cross-links in Fig. 3.3. Although the main behavior is very similar to that of the HFE cross-linker model, the use of the more realistic WLC force-extension curve has introduced a considerable smoothing of the cross-over. The nonlinear behavior in the WLC force-extension curve initiates slowly well before full extension, resulting in a more gradual onset of nonlinear behavior of the model with

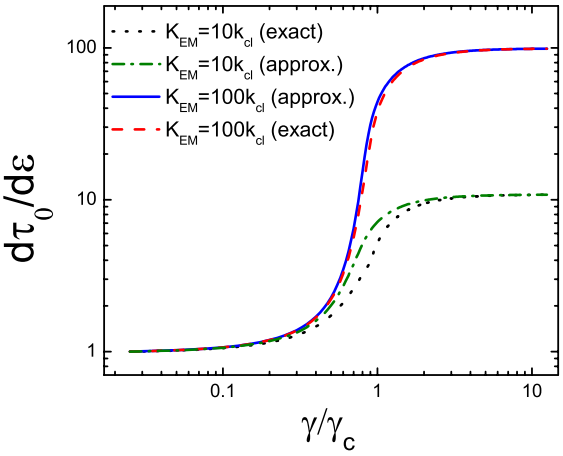

Figure 3.4 – (Color online) The 1D differential modulus $d\tau_0/d\epsilon$ of the rod with WLC cross-linkers as a function of the extensional strain ϵ imposed on the medium parallel to the orientation of the rod. The red dashed and black dotted curves show exact calculations using Eqs. (3.1) and (3.2) and the solid blue and green dash-dotted curves show approximate calculations using Eq. (3.7).

WLC cross-linkers. Importantly, the characteristic strain ϵ_c for the nonlinear behavior is proportional to ℓ_0/L, independent of the exact nonlinear response of the linkers.

For a calculation of network mechanics the average tension $\bar{\tau}$ in a filament is more relevant than the midpoint tension [35]. $\bar{\tau}$ is found by averaging the tension profile given by Eq. (3.3) along the backbone of the filament. The ratio $\bar{\tau}/\tau_0$ is shown in the inset of Fig. 3.3. We find that over a broad range of strains $\bar{\tau} = 3/2\tau_0$. During the cross-over regime the ratio exhibits a peak with an amplitude that depends on the exact ratio of K_{EM} and k_{cl}.

3.4 Self-Consistent medium model

The linear treatment of the effective medium breaks down at large strains; here the network exhibits a nonlinear response as the cross-linkers get extended into their nonlinear regime. Thus, it is no longer appropriate to describe that the effective medium, which should reflect the network elasticity, as linear. In this section we extend our model by requiring that the elasticity of the background medium *self-consistently* represents the nonlinear elasticity of the constituent BEU's. Within this approach, the elasticity of the medium depends on the density of filaments and on the elasticity of a BEU averaged over all orientations. The stiffness of the effective

medium K_{EM} that couples to a single cross-link is determined by the stiffness of a BEU

$$K_{EM} = \frac{\alpha}{nL}\frac{d\tau_0}{d\epsilon}. \tag{3.8}$$

The proportionality constant α may depend on the detailed structure of the network, and may be considered as a phenomenological coupling parameter between a linker and the surrounding network. In section 3.4.1 we estimate α using a continuum approach. The midpoint tension in a rod can be written in a similar form as Eq. (3.7)

$$\tau_0(\epsilon) = \frac{n}{L}\int^{\frac{L}{2}} dx'\, x' \int^{\epsilon} d\epsilon' \frac{k_{cl}(x'\epsilon')\frac{\alpha}{nL}\frac{d\tau}{d\epsilon}(\frac{x'\epsilon'}{L/2})}{k_{cl}(x'\epsilon') + \frac{\alpha}{nL}\frac{d\tau}{d\epsilon}(\frac{x'\epsilon'}{L/2})}, \tag{3.9}$$

where $k_{cl}(u)$ is the derivative of the force-extension relation of the cross-linker. Note that we have applied the same approximation as in Eq. (3.7). Eq. (3.9) can be simplified to the following differential equation for $\tau_0(\epsilon)$

$$2\frac{d\tau_0}{d\epsilon} + \epsilon\frac{d^2\tau_0}{d\epsilon^2} = \begin{cases} \frac{nL}{4}\frac{k_{cl}(\epsilon L/2)\frac{\alpha}{Ln}\frac{d\tau_0}{d\epsilon}}{k_{cl}(\epsilon L/2)+\frac{\alpha}{Ln}\frac{d\tau_0}{d\epsilon}} & \text{if } \epsilon < \frac{\ell_0}{L/2} \\ \frac{\alpha}{4}\frac{d\tau_0}{d\epsilon} & \text{if } \epsilon \geq \frac{\ell_0}{L/2} \end{cases} \tag{3.10}$$

We find the following behavior of this model with WLC cross-linkers. Below the characteristic strain for nonlinear response $\epsilon_c = 2\ell_0/L$, the tension in a rod depends approximately linearly on strain. This linearity will be reflected in the self-consistent effective medium, and the model will exhibit a behavior similar to the linear medium model up to the critical strain. By solving Eq. (3.10) we find the midpoint tension τ_0 in a rod as a function of extensional strain ϵ. Beyond the critical strain the tension depends highly nonlinearly on strain, with a derivative that increases as

$$\frac{d\tau_0}{d\epsilon} \sim \epsilon^{\frac{\alpha}{4}-1}. \tag{3.11}$$

Note that unlike in the linear medium model, where the derivative asymptotes to a final value set by K_{EM}, here $d\tau_0/d\epsilon$ increases indefinitely. For the HFE cross-linkers we find similar behavior, although in that case the cross-over between the linear regime and the asymptotic stiffening regime is more abrupt.

3.4.1 Continuum elastic limit

Here we derive an expression for the coupling parameter α in the continuum elastic limit. Note that this will only be a good approximation for a dense, isotropic network.

The modulus of the medium G_{EM} can be expressed in terms of the stiffness $\frac{d\tau_0}{d\epsilon}$ of a BEU by averaging over rod orientations [36]

$$G_{\text{network}} = \frac{1}{15}\rho\frac{d\bar{\tau}}{d\epsilon}, \tag{3.12}$$

where ρ is the length of filament per unit volume. ρ can also be expressed in terms of the mesh-size $\rho = 1/\xi^2$. In the linear medium treatment in section 3.3 we found that $\bar{\tau} = \frac{2}{3}\tau_0$. Thus, the network modulus reads

$$G_{\text{network}} = \frac{2}{45}\frac{1}{\xi^2}\frac{d\tau_0}{d\epsilon}. \tag{3.13}$$

We proceed by relating K_{EM} to G_{network}, which enables us to find an expression for α. Consider a rigid rod of diameter a and length L, which we use as a microrheological probe in an effective elastic medium with a shear modulus G_{EM}. If the rod is displaced along its axis, it will induce a medium deformation $\delta\ell$ that leads to a restoring force acting along its backbone. The restoring force per unit length is given by $2\pi G_{EM}/\log(L/a) \times \delta\ell$. Here we ignore the log term, which is of order 2π. Thus, the stiffness of the medium per cross-link K_{EM} is related to G_{EM} by

$$K_{EM} = \frac{L}{n}G_{EM}. \tag{3.14}$$

By requiring $G_{EM} = G_{network}$ we find α from Eqns. (3.13) and (3.14)

$$\alpha = \frac{2}{45}\left(\frac{L}{\xi}\right)^2. \tag{3.15}$$

Note that for a dense network $\alpha \gg 1$.

3.5 3D Network calculation

In this section we describe in detail how the macroscopic mechanical properties of a uniformly deforming network can be inferred from single filament properties. This procedure has been used to describe the viscoelastic [36] and nonlinear elastic properties [4, 5, 8] of semiflexible polymer networks with point-like rigid cross-links; here we present a detailed derivation of this theory. The main assumption of this calculation is a uniform, or affine deformation of the network. An affinely deforming polymer chain of length ℓ will stretch or compress, depending on its orientation, by an amount that scales as $\sim \ell\gamma$. The validity of the affine treatment of cross-linked semiflexible polymer networks has been subject to much debate. Simulations of networks in 2D demonstrate that the deformation can be both affine and non-affine depending on

the density of the network and filament rigidity [32, 33]. Here we derive the affine theory for the case of a filamentous network with point-like rigid cross-links. Then we show how this framework can be used together with the effective medium approach to describe the mechanics of stiff polymer networks with flexible cross-links.

Consider a segment of a filament between two cross-links with an initial orientation $\hat{n}$. When subjected to a deformation described by the Cauchy deformation tensor Λ_{ij}, this filament segment experiences an extensional strain directed along its backbone

$$\epsilon = |\Lambda\hat{n}| - 1. \tag{3.16}$$

As before, we denote a 1D extensional strain with ϵ and a 3D strain with γ. This extensional strain leads either to compression or extension in the polymer segment depending on its orientation, and thus results in a tension $\tau(|\Lambda\hat{n}| - 1)$. The contribution of this tension to the macroscopic stress depends also on the orientation of the polymer segment. By integrating over contributions of the tension over all orientations accordingly, we can compute the macroscopic stress tensor σ_{ij}. The contribution of the tension in a polymer segment with an initial orientation $\hat{n}$ is calculated as follows. The deformation Λ_{ij} transforms the orientation of the segment into $n'_j = \Lambda_{jk}n_k/|\Lambda\hat{n}|$. Thus, the length density of polymers with an orientation $\hat{n}$ that cross the j-plane is given by $\frac{\rho}{\det\Lambda}\Lambda_{jk}n_k$, where the factor $\det\Lambda$ accounts for the volume change associated with the deformation. For the network calculations in this chapter we consider only simple shear, which conserves volume ($\det\Lambda = 1$). The tension in the i-direction in a filament with an initial orientation $\hat{n}$, as it reorients under strain, is $\tau(|\Lambda\hat{n}| - 1)\Lambda_{il}n_l/|\Lambda\hat{n}|$. Thus, the (symmetric) stress tensor reads [5]

$$\sigma_{ij} = \frac{\rho}{\det\Lambda}\left\langle \tau(|\Lambda\hat{n}| - 1)\frac{\Lambda_{il}n_l\Lambda_{jk}n_k}{|\Lambda\hat{n}|}\right\rangle. \tag{3.17}$$

The angular brackets indicate an average over the initial orientation of the polymer chains.

One important feature follows directly from Eq. (3.17). A nonlinear force extension curve for the filaments is not strictly required for a nonlinear network response. The extensional strain of a filament depends nonlinearly on the macroscopic strain of the network,

$$\epsilon = \sqrt{1 + 2\gamma_{kl}\hat{n}_k\hat{n}_l} - 1. \tag{3.18}$$

Furthermore, the reorientation of the filaments under strain leads to an increasingly more anisotropic filament distribution. These geometric effects result in a stiffening of the shear modulus under shear strains of order 1, even in the case of linear Hookean filaments. At large strains all filaments are effectively oriented in the strain direction, which limits the amount of stiffening to a factor of 4 (2D networks) and 5 (3D networks) over the linear modulus in the large strain limit. Thus the stiffening

due to this effect occurs only at large strains and is limited. Therefore, we expect this mechanism to have a marginal contribution to the more dramatic stiffening that is observed in biopolymer gels at strains < 1 [4,5]. We would like to stress that the geometric stiffening discussed above has a different nature than the geometric stiffening discussed by [29,37]. In their case, the stiffening is attributed to a cross-over between an elastic response dominated by soft bending modes in the zero strain limit and a stiffer stretching mode dominated regime at finite strains. In the affine calculation described here, only stretching modes are considered.

By limiting ourself to a small strain limit, we exclude the geometric stiffening effects discussed above. This is instructive, since it allows us to study network stiffening due to filament properties alone, and it is a good approximation for most networks since the nonlinear response typically sets in at strains < 1. For a volume conserving deformation ($\det\Lambda = 1$) in the small strain limit the stress tensor in Eq. (3.17) reduces to [36]

$$\sigma_{ij} = \rho \left\langle \tau(\gamma_{kl}\hat{n}_k\hat{n}_l)\hat{n}_i\hat{n}_j \right\rangle, \tag{3.19}$$

In this limit the geometric stiffening mechanism discussed above is absent. Next we show explicitly how to calculate the shear stress σ_{xz}, in the z-plane for a network, which is sheared in the x-direction. A filament segment with an orientation given by the usual spherical coordinates θ and φ undergoes an extensional strain

$$\begin{aligned} \epsilon &= \sqrt{1 + 2\gamma\cos(\varphi)\sin(\theta)\cos(\theta) + \gamma^2\cos^2(\theta)} - 1 \\ &\approx \gamma\cos(\varphi)\sin(\theta)\cos(\theta), \end{aligned} \tag{3.20}$$

where we have used a small strain approximation in the second line. The tension in this segment contributes to the xz-component of the stress tensor through a geometric multiplication factor $\cos(\phi)\sin(\theta)\cos(\theta)$, where the first two terms are due to a projection of the forces in the x-direction and the second term is due to a projection of the orientation of the filament into the orientation of the z-plane. The stress in the xz-direction is thus given by

$$\sigma_{xz} = \frac{\rho}{4\pi}\int_0^{\pi}\int_0^{2\pi} d\theta d\varphi\ \sin(\theta)\tau\left[\gamma\cos(\varphi)\sin(\theta)\cos(\theta)\right]\cos(\varphi)\sin(\theta)\cos(\theta). \tag{3.21}$$

Since we limit ourselves to the small strain limit, we do not account for a redistribution of the filament orientations by the shear transformation in this equation.

3.5.1 Semiflexible polymer networks with rigid point-like cross-links

In this section we discuss how the affine framework can be used to compute the elastic response of a network with inextensible semiflexible polymers connected by point-like

rigid cross-links.

Consider a segment of an inextensible semiflexible polymer of length ℓ_c between two rigid cross-links in the network. Thermal energy induces undulations in the filament, which can be stretched out by an applied tension. Within the WLC model in the semiflexible limit $\ell_c \gtrsim \ell_p$, the force-extension relation of this segment has been shown to be given implicitly by [28]

$$\delta\ell = \frac{\ell_c^2}{\pi^2 \ell_p} \sum_{n=1}^{\infty} \frac{\phi}{n^2(n^2+\phi)}, \tag{3.22}$$

where ϕ is the tension τ normalized by the buckling force threshold $\kappa\frac{\pi^2}{\ell_c^2}$. This relationship can be inverted to obtain the tension as a function of the extension $\delta\ell$:

$$\tau = \kappa \frac{\pi^2}{\ell_c^2} \phi\left(\delta\ell/\delta\ell_{\max}\right), \tag{3.23}$$

where $\delta\ell_{\max} = \frac{1}{6}\ell_c^2/\ell_p$ is the total stored length due to equilibrium fluctuations. This is also the maximum extension, which can be found from Eq. (3.22) as $\phi \to \infty$. For small extensions $\delta\ell$ this reduces to

$$\tau = 90 \frac{\kappa^2}{k_B T \ell_c^4} \delta\ell. \tag{3.24}$$

This result can be inserted into Eq. (3.19) to find the linear modulus of the network

$$G_0 = 6\rho \frac{\kappa^2}{k_B T \ell_c^3}. \tag{3.25}$$

For a network in either two or three dimensions, the maximally strained filaments under shear are oriented at a 45 degree angle with respect to the shear plane, implying that the maximum shear strain is

$$\gamma_{\max} = \frac{1}{3}\frac{\ell_c}{\ell_p}. \tag{3.26}$$

Using the small strain approximation(as in Eq. (3.19)), we can calculate the nonlinear network response

$$\begin{aligned} \frac{\sigma}{\sigma_c} &= \frac{1}{4\pi}\int_0^{\pi}\int_0^{2\pi} d\theta d\varphi \, \sin(\theta)\{ \\ &\phi\ \left[\tilde{\gamma}\cos(\varphi)\sin(\theta)\cos(\theta)\right]\cos(\varphi)\sin(\theta)\cos(\theta)\} \end{aligned} \tag{3.27}$$

where we define the critical stress to be $\sigma_c = \rho\frac{\kappa}{\ell_c^2}$. We have also defined $\tilde{\gamma} = \gamma/\gamma_c$, where the critical strain for the network is given by

$$\gamma_c = \frac{1}{6}\frac{\ell_c}{\ell_p}. \tag{3.28}$$

Eq. (3.27) demonstrates that the nonlinear response of a network of inextensible semiflexible polymers with rigid cross-links is universal for small strains [4]. Note, however, that this would not hold if we would use the full nonlinear theory from Eq. (3.17), valid for arbitrarily large strains. Thus, geometric stiffening effects may lead to small departures from universality. Alternatively, universality may break down as a result of enthalpic stretching of the polymer backbone [5]. The universal nonlinear elastic response for a semiflexible polymer network with rigid cross-links is shown in Figs. 3.5 and 3.6. The divergence of the differential modulus beyond the critical strain is of the form $\sim \frac{1}{(1-\gamma_{\max})^2}$, as depicted in Fig. 3.5. This results into a powerlaw stiffening regime of the form $K \sim \sigma^{3/2}$, as shown in the inset of Fig. 3.6. This prediction is consistent with experiments on actin gels with the rigid cross-linker scruin [4].

In this section we have assumed that at zero strain all filament segments are at their equilibrium zero-force length. However, cross-linking of thermally fluctuating polymers will result in cross-linking distances both smaller and greater than their equilibrium length. This effect, which is ignored in our discussion here, leads to internal stresses build into the network during the gelation [5].

3.5.2 Stiff polymer networks with highly flexible cross-links

For a network with flexible cross-links we do not consider the tension in filament segments, but rather the average tension $\bar{\tau}$ in the whole filament. By using the effective medium approach we can compute the average tension in a filament as a function of the orientation of the rod and the macroscopic shear strain γ. Contributions to the stress from the average tension in the rods are integrated over all orientations according to Eq. (3.21). In our description we thus assume affine deformation of the network on length scales $> L$. Note, however, that we do not assume that the cross-links deform affinely.

We find both from the linear medium model and the self-consistent model for a network with highly flexible cross-links that the linear modulus is approximately given by

$$G_0 \approx \frac{1}{8}\rho n k_{cl} L. \tag{3.29}$$

The appearance of the filament length L in this equation is remarkable, and is due to the non-uniform deformation profile of the cross-links, which leverages the forces applied by the cross-links further from the midpoint of the filament. The onset of nonlinear elastic response occurs at a critical strain

$$\gamma_c = 4\frac{\ell_0}{L}. \tag{3.30}$$

The full nonlinear response as predicted by our model is shown in Figs. 3.5 and 3.6. The results of the linear medium model with WLC cross-links, as shown with a green dotted line, are qualitatively similar to the results of the 1D model (see Fig. 3.3). For the self-consistent model we find that beyond γ_c the differential modulus increases as a powerlaw, as shown in Fig. 3.5. There appears to be only a small quantitative difference between the model with HFE and WLC cross-links.

The differential modulus $K = d\sigma/d\gamma$ is plotted as a function of stress in Fig. 3.6. The stress is normalized by the critical stress σ_c, which we define here as

$$\sigma_c = G_0\gamma_c = \frac{1}{2}\rho n k_{cl}\ell_0. \tag{3.31}$$

We find a sharp increase in stiffness beyond the critical stress, which quickly asymptotes to a powerlaw regime, where the exponent is given by $1 - 1/(\frac{1}{60}(L/\xi)^2 - 1)$. Interestingly, this exponent does not depend on the exact form of the nonlinear response of the cross-linkers. This exponent emerges as a consequence of the finite extendability of the cross-links and the non-uniform deformation profile along the backbone of the filament. In the dense limit we consider in our model, the deviation from an exponent of 1 is small and depends only weakly on the ratio L/ξ. As an example, we consider a typical *in vitro* network for which $\xi = 0.3$ μm and the average filament length $L = 15$ μm, for which we find an exponent of 0.98. The asymptotic powerlaw regime with an exponent ≈ 1, as predicted by our model is consistent with recent experimental data on actin networks cross-linked by filamin [11, 16]. Finally, the inset of Fig. 3.6 shows the rigid linker model together with the self-consistent model for a network with flexible cross-links. In this case the stress is normalized by a stress σ_0, which marks the knee of the curve.

3.6 Tension profiles and single cross-linker force estimate

Recently, there has been much debate on the mechanical response of actin binding proteins such as filamin. Specifically, it is discussed whether the cross-links stiffen, unfold or unbind under tension in both physiological or *in vitro* conditions. The precise response of the linkers may have implications for the dynamical and mechanical properties of the cytoskeleton. The discussion has been partially resolved recently by single molecule [27] and bulk rheology [16] experiments on the actin-filamin system. These experiments indicate that cross-links unbind at forces well below the force required for domain unfolding. It is helpful for the interpretation bulk rheology experiments to be able to infer the forces experienced by a single cross-linker from the measured mechanical stress. In this section we show that by using the shape of

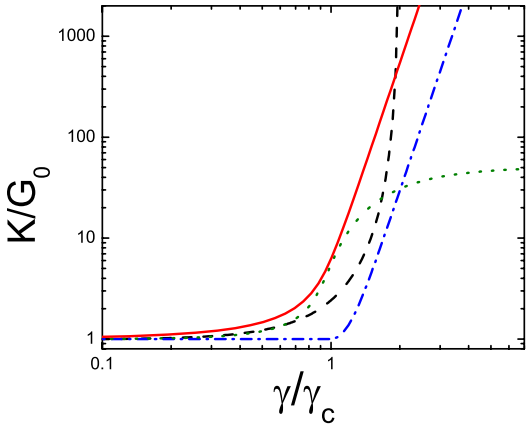

Figure 3.5 – (Color online) The differential modulus $K = d\sigma/d\gamma$ normalized by the linear modulus G_0 as a function of strain normalized by the critical strain γ_c. The universal curve for a semiflexible polymer network with rigid cross-links is shown as a black dashed curve. We also show the results of the self-consistent model with WLC cross-links (red solid curve) and simple cross-links (blue dash-dotted curve), the linear medium model with WLC cross-links with $K_{EM} = 100k_{cl}$ (green dotted curve).

the tension profile, we can relate a macroscopic quantity such as the stress to the maximum force experienced by a single cross-linker in the network.

The tension along a single filament is not uniform in networks of stiff finite length filaments and incompliant cross-links [32, 38]. It was found in simulations that in the affine regime the tension profile is flat close to the midpoint and the tension decreases exponentially towards the boundaries of the filament. In the non-affine regime a different tension profile has been reported, in which the tension decreases linearly towards the ends [38]. In the case of a flexibly cross-linked network of stiff polymers we also expect a non-uniform tension profile, although in this case the underlying physics is different. The deformation of a cross-linker at a distance x from the midpoint of the rod is $u_{cl} \sim x\gamma$; thus, cross-links further away from the midpoint exert larger forces on the rod, resulting in a non-uniform tension profile.

We can calculate the tension profile for a given rod using Eq. (3.3). In the limit of highly flexible cross-linkers, the tension profile in the linear elastic regime is given by

$$\tau(\epsilon, x) = \frac{n}{L}\frac{k_{cl}K_{EM}}{k_{cl}+K_{EM}}\frac{1}{2}\left(x^2 - \left(\frac{L}{2}\right)^2\right)\epsilon. \tag{3.32}$$

The tension profiles as computed with the self-consistent model with WLC cross-links are shown for various strains in Fig. 3.7. For low strains we find a parabolic profile, which flattens out towards the edges for larger strains.

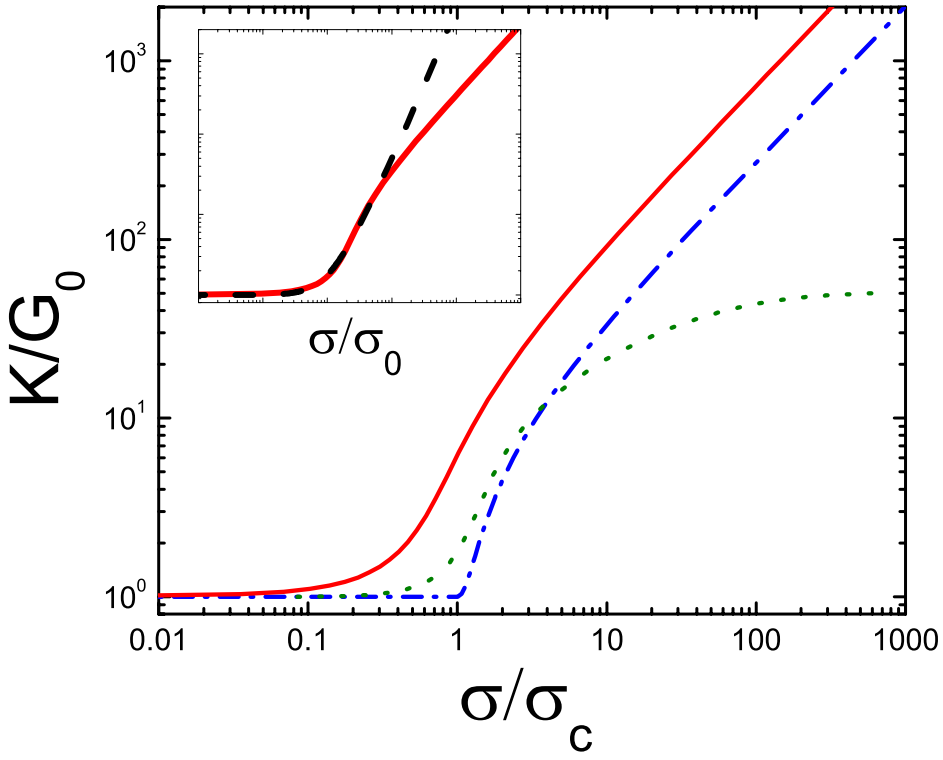

Figure 3.6 – (Color online) The differential modulus $K = d\sigma/d\gamma$ normalized by the linear modulus G_0 as a function of stress normalized by the critical stress σ_c for the self-consistent model with WLC cross-links (red solid curve), HFE cross-links (blue dash-dotted curve) and the linear medium model with WLC cross-links with $K_{EM} = 100k_{cl}$ (green dotted curve). The inset shows the rigid linker model together with the self-consistent model for a network with flexible cross-links. In this case the stress is normalized by a stress σ_0, which marks the knee of the curve.

We now proceed to estimate the force experienced by a single cross-linker. For an affinely deforming network in the linear response regime Eq. (3.17) simplifies to

$$\sigma = \frac{1}{15}\rho\,\bar{\tau}(\gamma). \tag{3.33}$$

Filaments at a 45° angle with respect to the stress plane bear the largest tension $\bar{\tau}_{max}$ and experience a strain along their backbone of $\gamma/2$. Assuming linear response we find $\bar{\tau}_{max}(\gamma) = \bar{\tau}(\gamma)/2$. In the case of a parabolic tension profile, the average tension $\bar{\tau}$ in a filament is related to the largest force f_0 experienced by a cross-linker at the boundary of the rod by $\bar{\tau} = \frac{1}{6}nf_0$. Thus, we can express the macroscopic stress in terms of the maximum forces experienced by cross-linkers on the filaments under the greatest load

$$\sigma = \frac{1}{45}\rho n f_{max}. \tag{3.34}$$

For the derivation of this equation we have assumed to be in the linear response regime. In the nonlinear regime we expect the expression to still hold approximately, although the prefactor will change.

Recently, Kasza et al. [16] found that the failure stress of the network σ_{max} is proportional to the number of cross-links per filament n in actin networks with the flexible cross-linker filamin. This suggests that filamin failure, rather than rupture of single actin filaments is the cause for network breakage. In contrast, for actin networks with the rigid cross-linker scruin, which binds more strongly to actin than filamin, rupture of actin was found to be the mechanism for network failure [4]. On the basis of our model and the experimental data from Ref. [16] we estimate filamin failure forces of order $1-5$ pN, far below the unfolding force 100 pN. This suggests that network failure is due to filamin unbinding. This is consistent with recent single molecule experiments, which show that filamin unbinding is favored over unfolding of the Ig-domains for low loading rates [27].

These numerical estimates for the force experienced by a single filamin cross-linker are for *in vitro* conditions. Under such conditions actin is present with a concentration of ~ 1 mg/ml and filamin is present at an actin to filamin ratio of ~ 100. *In vivo* the concentration of actin is believed to be an order of magnitude larger [16]. Living cells are, however, under stresses which in some cases are found to be of order 1000 Pa [42], more than an order magnitude larger than in the *in vitro* systems [11,16]. Hence, the forces experienced by an individual cross-linker *in vivo* will be of the same order of magnitude as under *in vitro* conditions. Therefore, we do not expect a significant amount of domain unfolding of filamin to occur *in vivo* under typical conditions.

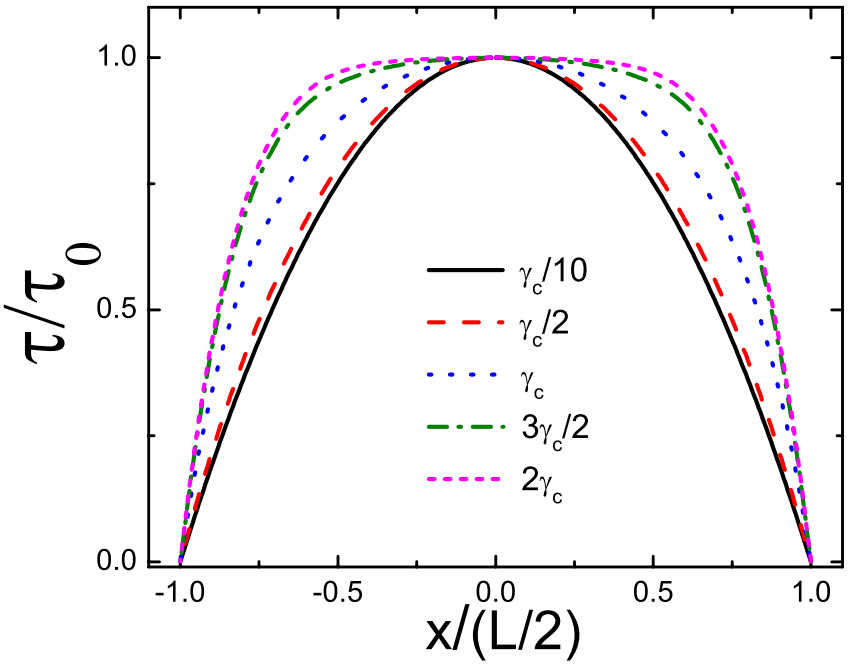

Figure 3.7 – (Color online) The reduced tension profile along the rod, normalized by the midpoint tension τ_0. This profile is calculated with the self-consistent model with WLC cross-links.

3.7 Implications and discussion

We have studied the nonlinear elasticity of stiff polymer network with highly flexible cross-links. We find that the mechanics of such a network is controlled by network connectivity expressed in terms of the number of cross-links per filament n. This was found earlier in experiments on actin-filamin gels [16], providing strong experimental evidence for cross-link dominated mechanics in these networks. Within this picture, stiffening occurs at a strain where the cross-links are stretched towards their full extension. As a result, we expect γ_c to be proportional to the molecular weight of the cross-linker ℓ_0. This prediction is consistent with the results of Wagner et al. [12], where cross-link length was varied, while keeping the average filament length fixed. Interestingly, they observed larger values of γ_c than expected either from our model or based on Refs [11, 12, 16].

In addition, we find here that the filament length L plays an important role in the nonlinear elasticity of these networks. In particular, the onset of nonlinear response $\gamma_c \sim \ell_0/L$ depends crucially on filament length. This has been confirmed by recent experiments on actin-filamin gels, showing an approximate inverse dependence of the γ_c on actin filament length [16]. The sensitivity of network response to filament length, both in experiments and in our model, appears to be one of the hallmarks of actin-filamin networks. On the one hand, this may explain the apparent difference between the critical strains reported in Refs. [11, 12, 16]. On the other hand, this also suggests that it may be even more important in such flexibly cross-linked networks to directly control and measure the filament length distribution than for other *in vitro* actin studies [39]. Our model does not account for filament length polydispersity. A distribution in filament length is expected to smooth somewhat the sharp stiffening transition predicted by our model.

The dependence of the critical strain for networks with flexible cross-links observed in experiments and predicted by our model is in striking contrast with the behavior found for rigidly cross-linked networks. In the latter case, theory predicts $\gamma_c \sim \ell_p/\ell_c$ (see Eq. (3.28)) consistent with experimental observations [4]. The insensitivity of the nonlinear elasticity of dense networks cross-linked with rigid linkers to filament length would suggest that network mechanics cannot be effectively controlled by actin polymerization regulation. We have shown here that the filament length plays a crucial role for networks with flexible cross-links, which are abundant in the cellular cytoskeleton. Thus regulating actin length by binding/capping proteins such as gelsolin may enable the cell not only to sensitively tune its linear elastic modulus, but also the onset of the nonlinear response of its cytoskeleton.

In the nonlinear regime we expect the differential modulus to increase linearly with stress for a dense flexibly cross-linked network. This behavior is a direct consequence of the non-uniform deformation profile along a filament and the finite ex-

tendability of the cross-links, although it is independent of the exact shape of the force-extension behavior of the cross-links. The powerlaw stiffening $K \sim \sigma^y$ with $y \approx 1$ is consistent with recent experiments on actin-filamin gels [11, 16]. This stiffening behavior is very different from the nonlinear response observed for actin gels with rigid cross-links for which a powerlaw exponent of 3/2 is observed [4], consistent with theory for an affine response governed by the stretching out of thermal fluctuations of the actin filaments. Interestingly, *in vivo* experiments show that cells also exhibit power-law stiffening with an exponent of 1 [40].

In this chapter we examined a limit in which the stiffness of the cross-links is small compared to the stiffness of an F-actin segment between adjacent cross-links. For a large flexible cross-linker such as filamin this is clearly a good approximation in the linear regime. However, as the cross-links stiffen strongly they could, in principle, become as stiff as the actin segment. This would affect the nonlinear response of the network. To investigate this we calculated the differential stiffness df/du as a function of force f for a filamin cross-linker and an actin segment with a length 0.5 to 2 μm, spanning the range of typical distances between cross-links in dense and sparse networks respectively. This result is shown in Fig. 3.8. We that find the differential stiffness of a filamin cross-link is always smaller than for an F-actin segment, even at large forces in the nonlinear regime. This justifies our approach, in which we ignored the compliance of the actin, for a broad range of experimentally accessible polymer/cross-linking densities. However, at sufficiently high filamin concentrations, it may be possible that individual network nodes involve multiple cross-linkers, in which case the actin filament compliance may also become relevant. Thus the effect of the compliance of F-actin remains an interesting topic for further research.

We also use our model to study these networks on a more microscopic level, such as the non-uniform tension profiles along the filament backbone. These profiles can be used to establish a relation between the macroscopic stress and the largest force experienced by a single cross-linker in the network. This allows us to estimate the forces experienced by filamin cross-links under typical *in vitro* and *in vivo* conditions. We find that the load on these cross-links is not sufficiently high to lead to significant domain unfolding of the filamin Ig-domains, even at stresses large enough to rupture the network. Indeed both rheology experiments on actin filamin gels and single molecule experiments indicate that unbinding occurs well before domain unfolding.

In other large flexible cross-links such as spectrin [41], domain unfolding occurs at lower, more relevant forces. In this case the domain unfolding could have a dramatic effect on the nonlinear viscoelasticity of such networks. In previous work, DiDonna and Levine simulated 2D cross-linked networks, where they assumed a sawtooth force-extension curve for the cross-linkers to mimic domain unfolding [13]. Their model, however, does not include the dramatic stiffening that is known to occur before unfolding in filamin cross-links. They observe a fragile state with shear

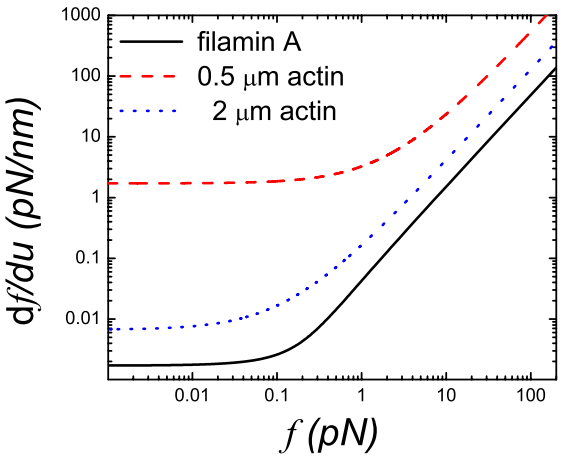

Figure 3.8 – (Color online) The differential stiffness df/du as a function of force f for a filamin cross-linker (solid line) and for several F-actin polymer segment lengths.

softening when an appreciable number of cross-linkers are at the threshold of domain unfolding. Our model is based on the stiffening of the cross-linkers, which initiates at forces far below those required for domain unfolding. This leads to strain stiffening at a point where only a fraction of cross-linkers are at their threshold for nonlinear response. Thus in both our model and that of Ref. [13] the network responds strongly to small strain changes, though in an opposite manner: stiffening in the present case vs softening in Ref. [13].

In related work, Dalhaimer, Discher, and Lubensky show that isotropic networks linked by large compliant cross-linkers exhibit a shear induced ordering transition to a nematic phase [14]. It would be interesting to investigate the effect of the nonlinear behavior of the cross-links on this transition. In the present calculation we have assumed an isotropic network. An ordering transition, which results in a strong alignment of filaments will dramatically affect the nonlinear elasticity of the network.

In this article we have studied networks of stiff polymers linked by highly flexible cross-links. Both experiments [11, 16] and our model [15] indicate that these networks have novel nonlinear rheological properties. We find that the network mechanics is highly tunable. By varying filament length, cross-linker length and network connectivity we can sensitively regulate the linear and nonlinear elasticity over orders of magnitude. These unique properties can be exploited in the design of novel synthetic materials.

3.8 Acknowledgments

This work was performed in collaboration with C. Storm. We thank K. Kasza, G. Koenderink, E. Conti and M. Das for helpful discussions.

Bibliography

[1] P. A. Janmey, U. Euteneuer, P. Traub, M. Schliwa. *Viscoelastic properties of vimentin compared with other filamentous biopolymer networks.* J. Cell Biol. **113**, 155 (1991).

[2] F. C. MacKintosh and P. A. Janmey. *Actin Gels*. Curr. Opin. Solid State Mater. Sci. **2**, 350 (1997).

[3] J. Y. Xu, D. Wirtz, T. D. Pollard. *Dynamic cross-linking by alpha-actinin determines the mechanical properties of actin filament networks*. J. Biol. Chem. **273**: 9570 (1998).

[4] M. L. Gardel, J. H. Shin, F. C. MacKintosh, L. Mahadevan, P. A. Matsudaira, and D. A. Weitz. *Elastic behavior of cross-linked and bundled actin networks*. Science **304**:1301-1305 (2004).

[5] C. Storm, J. Pastore, F. C. MacKintosh, T. C. Lubensky and P. A. Janmey. *Nonlinear elasticity in biological gels*. Nature **435**:191 (2005).

[6] A. R. Bausch and K. Kroy. *A bottom-up approach to cell mechanics*. Nature Phys. **2**, 231 (2006) .

[7] O. Chaudhuri, S. H. Parekh and D. A. Fletcher. *Reversible stress softening of actin networks*. Nature **445**: 295 (2007).

[8] P. A. Janmey, M. E. McCormick, S. Rammensee, J. L. Leight, P. C. Georges, and F. C. MacKintosh. *Negative normal stress in semiflexible biopolymer gels*. Nature Materials **6**, 48 (2007).

[9] F. Gittes, B. Schnurr, P. D. Olmsted, F. C. MacKintosh, and C. F. Schmidt. *Microscopic Viscoelasticity: Shear Moduli of Soft Materials Determined from Thermal Flucuations*. Phys. Rev. Lett. **79**, 3286 (1997).

[10] K. E. Kasza, A. C. Rowat, J. Liu, T. E. Angelini, C. P. Brangwynne, G. H. Koenderink and D. A Weitz. *The cell as a material*. Curr. Opin. Cell Biol. **19**:101-7 (2007).

[11] M. L. Gardel, F. Nakamura, J. H. Hartwig, J. C. Crocker, T. P. Stossel, and D. A. Weitz. *Prestressed F-actin networks cross-linked by hinged filamins replicate mechanical properties of cells*. Proc. Natl. Acad. Sci. **103**:1762-1767 (2006);
M. L. Gardel, F. Nakamura, J. Hartwig, J. C. Crocker, T. P. Stossel, and D. A. Weitz. *Stress-dependent elasticity of composite actin networks as a model for cell behavior*. Phys. Rev. Lett. **96**:088102 (2006).

[12] B. Wagner, R. Tharmann, I. Haase, M. Fischer and A.R. Bausch. *Cytoskeletal polymer networks: The molecular structure of cross-linkers determines macroscopic properties*. Proc. Nat. Acad. Sci. USA **103**, 13974 (2006).

[13] B. A. DiDonna, and A. J. Levine. *Filamin Cross-Linked Semiflexible Networks: Fragility under Strain*. Phys. Rev. Lett. **97**, 068104 (2006).

[14] P. Dalhaimer, D. E. Discher and T. C. Lubensky. *Crosslinked actin networks show liquid crystal elastomer behaviour, including soft-mode elasticity* Nature Phys. **3**, 354 (2007).

[15] C. P. Broedersz, C. Storm, and F. C. MacKintosh. *Nonlinear elasticity of composite networks of stiff biopolymers with flexible linkers*. Phys. Rev. Lett. **101**:118103 (2008); C. P. Broedersz, C. Storm, and F. C. MacKintosh. *Effective-medium approach for stiff polymer networks with flexible cross-links*. Phys. Rev. E **79**:061914 (2009).

[16] K. E. Kasza, C. P. Broedersz, G. H. Koenderink, Y. C. Lin, W. Messner, E. A. Millman, F. Nakamura, T. P. Stossel, F. C. MacKintosh, D. A. Weitz. *Actin filament length tunes elasticity of flexibly crosslinked actin networks*. Biophys. J. **99**, 1091 (2010)

[17] C. Bustamante, J.F. Marko, E.D. Siggia and S. Smith. *Entropic elasticity of lambda-phage DNA*. Science **265**, 1599 (1994).

[18] J. F. Marko and E. D. Siggia. *Stretching DNA*. Macromolecules **27**, 981 (1995).

[19] J. Wilhelm and E. Frey. *Radial Distribution Function of Semiflexible Polymers*. Phys. Rev. Lett. **77**, 2581 (1996).

[20] A. Dhar and D. Chaudhuri. *Triple Minima in the Free Energy of Semiflexible Polymers*, Phys. Rev. Lett. **89**, 065502 (2002).

[21] J. Samuel and S. Sinha. *Elasticity of semiflexible polymers*. Phys. Rev. E **66**, 050801(R) (2002).

[22] S. Stepanow and G. M. Schutz. *The distribution function of a semiflexible polymer and random walks with constraints*. Europhys. Lett. **60**, 546 (2002).

[23] A. Ghosh, J. Samuel, and S. Sinha. *Elasticity of stiff biopolymers*. Phys. Rev E **76**, 061801 (2007).

[24] I. Schwaiger, A. Kardinal, M. Schleicher, A. Noegel and M. Rief. *A mechanical unfolding intermediate in an actin-crosslinking protein*. Nat. Struct. Biol. **11**, 81 (2003).

[25] S. Furuike, T. Ito, and M. Yamazaki. *Mechanical unfolding of single filamin A (ABP-280) molecules detected by atomic force microscopy*. FEBS Lett. **498**:72-75 (2001).

[26] Y. Tsuda, H. Yasutake, A. Ishijima, and T. Yanagida, Proc. Nat. Acad. Sci. USA **93**, 12937 (1996).

[27] M. Ferrer, H. Lee, J. Chen, B. Pelz, F. Nakamura, R. D. Kamm, and M. J. Lang *Measuring molecular rupture forces between single actin filaments and actin-binding proteins*. Proc. Natl. Acad. Sci. **105**, 9221-9226 (2008).

[28] F. C. MacKintosh, J. Käs, and P. A. Janmey. *Elasticity of semiflexible biopolymer networks*. Phys. Rev. Lett. **75**:4425-4428 (1995).

[29] P. R. Onck, T. Koeman, T. van Dillen, and E. van der Giessen. *Alternative explanation of stiffening in cross-linked semiflexible networks*. Phys. Rev. Lett. **95**, 178102 (2005).

[30] R. Tharmann, M. M. Claessens, and A. R. Bausch. *Viscoelasticity of isotropically cross-linked actin networks*. Phys. Rev. Lett. **98**:088103 (2007).

[31] J. S. Palmer and M. C. Boyce. *Constitutive modeling of the stress-strain behavior of F-actin filament networks*. Acta Biomaterialia, **4**, 597-612 (2008).

[32] D. A. Head, A. J. Levine, and F. C. MacKintosh. *Distinct regimes of elastic response and deformation modes of cross-linked cytoskeletal and semiflexible polymer networks*. Phys. Rev. E **68**:061907 (2003). (2003).

[33] J. Wilhelm and E. Frey. *Elasticity of Stiff Polymer Networks*. Phys. Rev. Lett. **91**, 108103 (2003).

[34] J. Liu, G. H. Koenderink, K. E. Kasza, F. C. MacKintosh, and D. A. Weitz. *Visualizing the Strain Field in Semiflexible Polymer Networks: Strain Fluctuations and Nonlinear Rheology of F-Actin Gels*. Phys. Rev. Lett. **98**, 198304 (2007).

[35] D. C. Morse. *Viscoelasticity of Concentrated Isotropic Solutions of Semiflexible Polymers. 1. Model and Stress Tensor*. Macromolecules **31**, 7030-7043 (1998).

[36] F. Gittes and F. C. MacKintosh. *Dynamic shear modulus of a semiflexible polymer network*. Phys. Rev. E **58**, R1241 (1998).

[37] C. Heussinger, B. Schaefer and E. Frey. *Nonaffine rubber elasticity for stiff polymer networks*. Phys. Rev. E **76**, 031906 (2007)

[38] C. Heussinger and E. Frey. *Force distributions and force chains in random stiff fiber networks*. Eur. Phys. J. E **24**, 47-53 (2007).

[39] P. A. Janmey , J. Peetermans, K. S. Zaner, T. P. Stossel, and T. Tanaka. *Structure and mobility of actin filaments as measured by quasielastic light scattering, viscometry, and electron microscopy*. J. Biol. Chem. **261**:8357-8362 (1986).

[40] P. Fernández, P. A. Pullarkat and A. Ott. *A Master Relation Defines the Nonlinear Viscoelasticity of Single Fibroblasts*. Biophys. J. **90**, 3796 (2006).

[41] M. Rief, J. Pascual, M. Saraste, H. E. Gaub. *Single molecule force spectroscopy of spectrin repeats: low unfolding forces in helix bundles*. J. of Mol. Biol. **286**, 553-561, (1999)

[42] N. Wang, I. M. Tolic-Norrelykke, J. Chen, S. M. Mijailovich, J. P. Butler, J. J. Fredberg and D. Stamenovic. *Cell Prestress. I. Stiffness and Prestress are Closely Associated in Adherent Contractile Cells*. Am. J. Physiol. **282**, C606 (2002).